Exploring the Chemical Space of C_3H_2NO Isomers and Bimolecular Reactions with Hydrogen Cyanide and Formaldehyde: Insights into the Emergence of Life

Sunanda Panda, Ayusman Chiranjibi, Devesh Awasthi, and Anakuthil Anoop*

Department of Chemistry, Indian Institute of Technology Kharagpur, 721302, West Bengal, India

E-mail: anoop@chem.iitkgp.ac.in

Abstract

The emergence of life remains one of the most intriguing scientific questions, and understanding the chemical processes that led to it is essential. Recent discoveries of C_3H_2NO isomers in the interstellar medium have motivated further exploration of this molecular formula. Here, we use density functional theory to explore the potential energy surface of C_3H_2NO isomers, including acyclic and cyclic structures, and identify twelve low-lying isomers. We then investigate bimolecular reaction with HCN and H_2CO using an artificial force-induced automated search and transition state search for the minimal energy routes. Our results predict the formation of Oxiran-2-ylazanide and (Z)2-aminoacetaldehyde as the kinetically and thermodynamically controlled products, respectively. These results provide insights into the potential formation of biomarkers such as N-methyleneformamide in the interstellar medium, which have been found in recent years. Our study contributes to prebiotic chemistry and offers a critical step toward understanding the chemical processes that led to the emergence of life in the universe.

Introduction

Understanding the chemical processes that gave rise to life on Earth and potentially elsewhere in the universe is a central question in astrobiology.[1–7] In this context, prebiotic molecules, which are precursors to biological molecules, are of particular interest.[8–14] The interstellar medium (ISM) is known to harbor a diverse range of organic molecules, including some prebiotic molecules.[15–17] Continuous advancements in observational and detection techniques have led to the discovery of an increasing number of molecules in the ISM.[18–23] With each new detection, our understanding of the complex chemistry in ISM deepens, shedding light on the potential formation pathways and astrobiological relevance of these molecules.[24,25]

Among the molecules detected in the ISM, glycolonitrile, also known as 2-hydroxy-amino-nitrile, has garnered attention due to its potential role as a prebiotic molecule and precursor to more complex organic compounds. Glycolonitrile has been involved in numerous reactions of significant prebiotic precursors. Schwartz and Goverde found that glycolonitrile acts as a promoter for HCN polymerization, along with cyanohydrin, which ultimately leads to the formation of nucleobases.[26] In addition to facilitating HCN oligomerization, glycolonitrile itself serves as a relevant prebiotic molecule, as it acts as a precursor to glycine,[27] which can give rise to adenine. It also acts as an intermediate for glycolic acid[27] formation, which eventually leads to adenine. Adenine can be produced directly by freezing dilute $HOCH_2CN$ solutions.[28] Thus, glycolonitrile plays a significant role as a precursor and catalyzes other precursors to form the building blocks of life. Recently glycolonitrile has been discovered in the interstellar medium, a region of space between stars containing gas and dust, of Sagittarius B2(N).[29] And several other isomers of glycolonitrile, such as HOCHCNH, OCH2CN, HOCHCN, HOCCNH, OCCNH, and OCCN, have been found in molecular clouds[30,31] by observing various rotational transitions of the molecules at radio wavelengths.

Another C_2H_3NO isomer found in the interstellar medium towards Sgr B2(N) and

IRAS 16293-2422,[32] as well as in the atmosphere of comet 67P/Churyumov-Gerasimenko, is methyl isocyanate. The ALMA radio telescope has tentatively identified N-methylene-formamide in interstellar space and more recently and confidently towards Sgr B2(N) and the star-forming region NGC 6334.[33] Due to its peptide linkage moiety, N-methylene-formamide can potentially aid in RNA formation.

The possible formation of achiral 3-membered and 4-membered N-heterocyclic molecules has also been suggested,[33] following the discovery of the first cyclic compound, cyclo-propenylidene, in the ISM.[34] Although rotational spectroscopy data indicate that hete-rocyclic compounds are less abundant than cyclic hydrocarbons,[35] their achiral nature makes them more reactive. This increased reactivity opens the door to more diverse reac-tions for the evolution of life.

The discovery of C_2H_3NO isomers highlights the potential for other structural ar-rangements of atoms with the same chemical formula. Studying these isomers and their formation in interstellar regions is, therefore, critical for understanding the chemical pro-cesses that occur in the universe and evaluating their potential to support life on other planets. Providing a comprehensive set of theoretically predicted geometries and their properties can aid in the identification and characterization of new molecules observed in the ISM. Theoritical studies have been performed for some of the well known biomarkers to investigate the energetics of all possible structural isomers. For example, pyrrole was the most stable C_4H_5N isomer due to its lowest standard enthalpy of formation among the eleven possible minima.[36] Additionally, a theoretical study on C_2H_5NO isomers was conducted to explore the diverse possibilities of structural arrangements and their rele-vance in prebiotic chemistry[37] with Spartan's conformer generation algorithm.[38,39]

A common approach for identifying novel molecules for a given molecular formula is to explore the chemical space with global optimization techniques. Commonly used global optimization methods include genetic algorithms,[40–43] which mimic the process of natural selection to search for the lowest energy isomers, and basin hopping algo-

rithms,[44–47] which explore the potential energy surface of molecules by making small structural changes. Such methods have been instrumental in investigating various biomarkers for specific chemical formulas, often identifying abundant species as the most stable isomers, as well as uncovering unexplored isomers for further investigation. For example, a comprehensive study of alanine and its isomers was performed by an isomer search algorithm, the random connection method.[48] The study proposed that the inherent stability of the α-amino nitrile, 2-aminopropanenitrile, is the dominant contributor to the common enantiomeric excess observed in α-amino acids.[48]

In addition to identifying possible isomers, understanding their formation processes is essential. Elucidating the reaction pathways and mechanisms that lead to the formation of these isomers can offer valuable insights into their stability, abundance, and roles in various environments, such as the interstellar medium or prebiotic chemistry. The classic Urey-Miller experiment involved mixing prebiotic molecules under electric sparks, leading to the formation of various amino acids. This experiment was simulated with *ab initio* molecular dynamics.[49] Vanka and coworkers demonstrated how HCN and water could be precursors to RNA and proteins, essential molecules in life.[50] More recently, Vanka's team synthesized HeH+ using the *ab initio* nanoreactor dynamics method, the first diatomic species ever to form in the universe.[51] Ochsenfeld and colleagues investigated prebiotically plausible RNA precursors using a modified nanoreactor method and automated post-simulation evaluation with RDKit and NetworkX analysis, examining their robustness at the GFN2-xTB level of theory.[52]

Another strategy employed to study prebiotic reactions involves using automated search methods based on transition state theory and artificial force-induced reactions.[53] For example, Nandi *et al.* investigated the HCN oligomerization pathway, a crucial process in chemical evolution, using an automated reaction search. They discussed the formation of dimers, trimers, and tetramers and proposed four thermal pathways leading to the formation of prebiotically relevant intermediates.[54] Similarly, Komatsu and Suzuki

employed this approach to identify a new reaction pathway that could lead to the formation of cytosine, an essential component of DNA and RNA molecules, in space.[55] In light of these studies, it is evident that exploring various computational approaches to simulate prebiotic reactions is essential for advancing our knowledge of the chemical processes that gave rise to life and understanding the formation pathways of these key molecules.

In our study, we employ both chemical space and reaction space search, namely global optimization and automated reaction search, to investigate the isomeric landscape of the C_2H_3NO molecular system and explore potential reactions between hydrogen cyanide (HCN) and formaldehyde (HCHO), both detected in the ISM. We chose HCN and HCHO for the automated reaction search procedure because they are among the first group of Miller intermediates and have been proposed to react in the formation of C_2H_3NO isomers such as glycolonitrile. Additionally, as some reaction pathways involving HCN and HCHO resulted in the formation of HNC, we also investigated binary reactions between HNC and HCHO. Several low-energy isomers predicted in our study have been detected in the ISM, such as methyl isocyanate, glycolonitrile, and N-methylene formamidine, which rank among the most stable isomers. The isomers we identified include cyclic and acyclic structures, with cyclic isomers primarily comprising N-heterocycles and O-heterocycles. Our findings offer valuable insights into prebiotic chemistry and provide calculated spectral data that may facilitate the future detection of these molecules.

Computational Details

Global optimization

We investigated the chemical space for C_2H_3NO using the ABCluster[56,57] program package. Local minima were optimized through the interface of the Gaussian 16[58] program. The RI[59]-PBE0[60]/def2-TZVP[61] level of theory, with D3BJ[62–64] dispersion correction, was employed for the geometry optimizations. Initially, we explored the potential energy sur-

face (PES) for the systems, generating 100 stationary points. We performed three different runs with a maximum of 100 cycles for different cube sizes. Subsequently, full geometry optimizations and frequency calculations for the low-lying isomers were performed using the RIJCOSX[65]-M062X[66,67]/def2-TZVP[61] level of theory, including the D3zero[68,69] dispersion correction, in the ORCA4.2.1[70] program package.

Reaction Search

We explored possible reactions using the PyAR[71,72] package. This method employs a tabu-search algorithm to generate various trial orientations of the reacting molecules and utilizes an artificial force[53] to facilitate the reaction. The artificial force parameter, represented as (γ), was set to values ranging from 1000 kJ mol^{-1} to 9000 kJ mol^{-1}. The number of trial geometries (N) was set to 32 for the initial run and then increased to 64 for the final run to ensure no additional reactions were found. Optimization incorporating the artificial force was carried out using the STATPT module of the Turbomole package[73] and the RI[59]-BP86[74]/def2-SVP[61] level of theory.

Optimization of Stationary Points: TS and Minima

We selected geometries of the endpoints from the trajectories generated by automated reaction search belonging to reactants and products. We conducted NEB-TS[75] calculations to locate the transition states. These initial geometries from NEB-TS[75] were utilized in transition state optimization followed by IRC[76] calculations. The two endpoints resulting from the IRC calculations were further optimized to validate the reactants and products. The absence of any imaginary frequencies confirmed the minima, whereas the presence of a single imaginary frequency verified the transition states. All NEB and optimization calculations were conducted using the ORCA4.2.1[70] package and the RIJCOSX[65]-M062X[66,67]/def2-TZVP[61] level of theory with D3zero[68,69] dispersion corrections. Subse-

quently, single-point calculations for the optimized geometries were further conducted using the DLPNO-CCSD(T)[77]/def2-TZVPP[78] level of theory. The Gibbs free energies were calculated at 158K, the temperature in the region of hot corino in IRAS 162932422.

Ab Initio Molecular Dynamics Simulation

We performed *ab initio* molecular dynamics (AIMD) simulations to assess the kinetic stability of the C_2H_3NO isomers obtained from the automated reaction search. These calculations were carried out using the ADMP[79–81] method, incorporated in the Gaussian 16[58,82] program . We conducted these simulations at 158K and 1 atm pressure. We selected these temperatures to represent the hot corino region in IRAS 16293-2422, room temperature, and a higher temperature, respectively, in order to examine the stability of the molecules under these conditions.

Roto-vibrational Constants

We calculated the roto-vibrational constants employing vibrational second-order perturbation theory (VPT2)[83] calculations based on the quartic force field (QFF) approach with the Gaussian 16[58,82] program package to obtain theoretical spectroscopic data of the products. The anharmonically corrected vibrational frequencies were computed using uwb97xd[84]/6-311++G[85,86] and uB3LYP[87,88]/6-311++G[85,86] level of theory as these methods were found relaible from various theoritical studies.

Results and Discussion

In this section, we present a comprehensive analysis of our findings on the C_2H_3NO molecular system. Our investigation begins with a discussion of isomers obtained through global optimization techniques. These isomers are categorized into stable molecules, reactive intermediates (diradicals, zwitterions), and dissociated molecular complexes. Next,

we explore the results from the automated reaction search, examining the molecules generated through reactions involving HCN with HCHO, as well as HNC with HCHO, in separate instances. Finally, we discuss the rotational constants of the identified isomers, providing valuable insights into their potential detection in the interstellar medium.

Global Optimization Search for C_2H_3NO Chemical Space

In our computational exploration of the chemical space of C_2H_3NO, encompassing possible isomers with two C, three H, one N, and one O atoms, we identified 48 distinct structural isomers. These are depicted in Figures 1-4, organized into the following categories: stable molecules with standard valency, diradicals, zwitterionic molecules, and dissociated molecules. Additionally, we present their relative energies (R.E.; kcal mol^{-1}) with respect to the most stable isomer–methylimino(oxo)methane or isocyanatomethane (**1**). The IUPAC names and SMILES strings are provided in the Supporting Information (Table S1).

The ten most stable isomers identified in our study are as follows. Methylimino(oxo)methane, or isocyanatomethane **1**, emerged as the most stable isomer. 2-Hydroxyacetonitrile **2**, commonly known as glycolonitrile and often associated with prebiotic chemistry, followed with a relative energy (R.E.) of 15.95 kcal mol^{-1} higher than isomer **1**. N-methyleneformamide (3) came next, exhibiting an R.E. of 22.55 kcal mol^{-1}. It is noteworthy that the well-known prebiotic molecule glycolonitrile **2** is not the most stable isomer among those we found from the global optimization.

Other notable isomers included 2-iminoacetaldehyde **4** and methylcyanate **5**, with relative energies of 24.19 and 26.94 kcal mol^{-1}, respectively. The 2-aminoethanolate **6** isomer also proved stable, with an R.E. of 28.66 kcal mol^{-1}. Several N and O heterocycles featured among the low-energy isomers discovered in this investigation, such as aziridin-2-one (**7**; R.E. = 35.05 kcal mol^{-1}), 1,3-oxazetidine (**8**; R.E. = 37.64 kcal mol^{-1}), oxirane-2-imine (**9**; R.E. = 40.82 kcal mol^{-1}), and 2H-azirin-3-ol (**10**; R.E. = 43.29 kcal mol^{-1}).

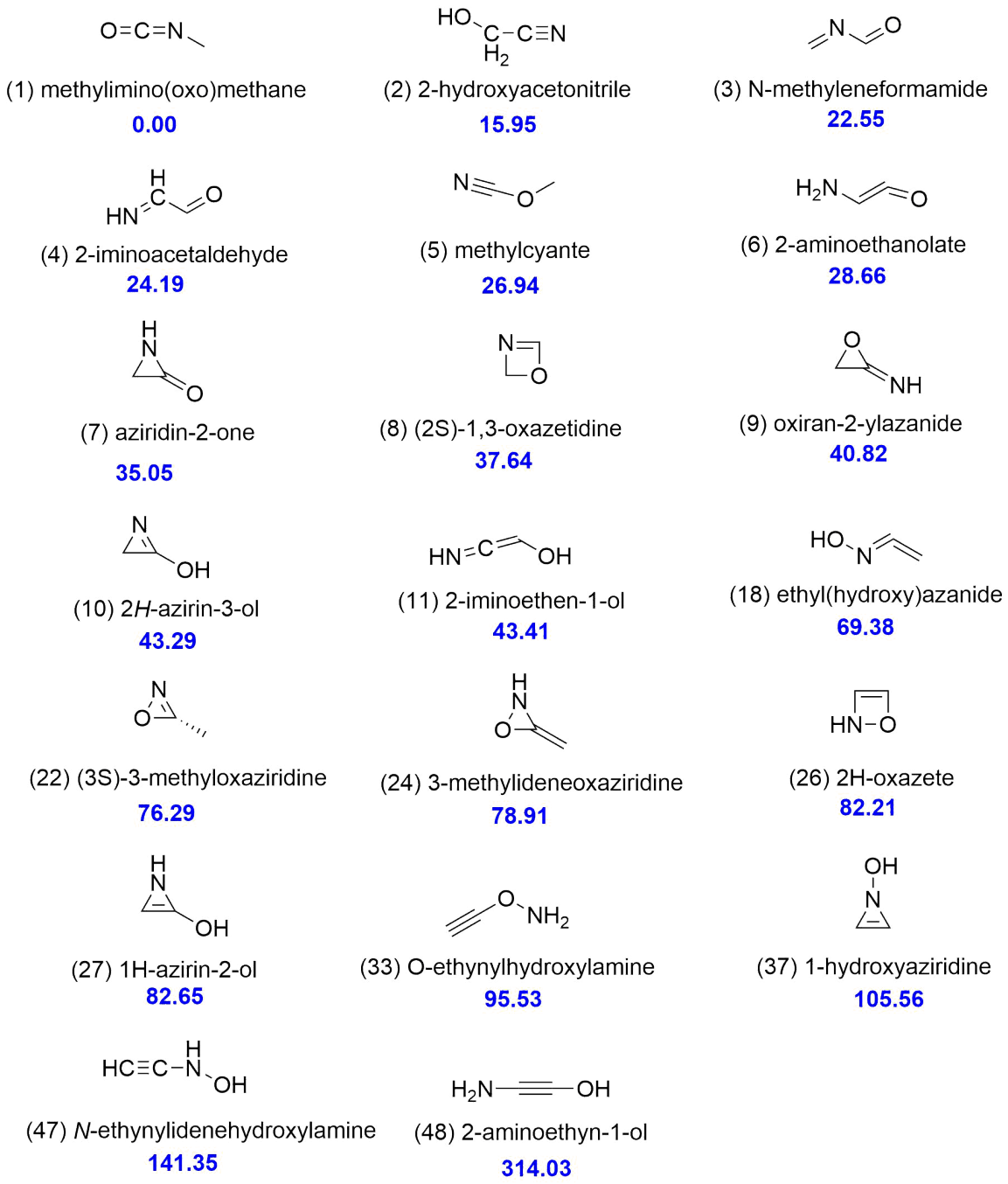

Figure 1: C_2H_3NO isomers with standard valency with their IUPAC name and relative energy in kcal mol^{-1} (in blue)

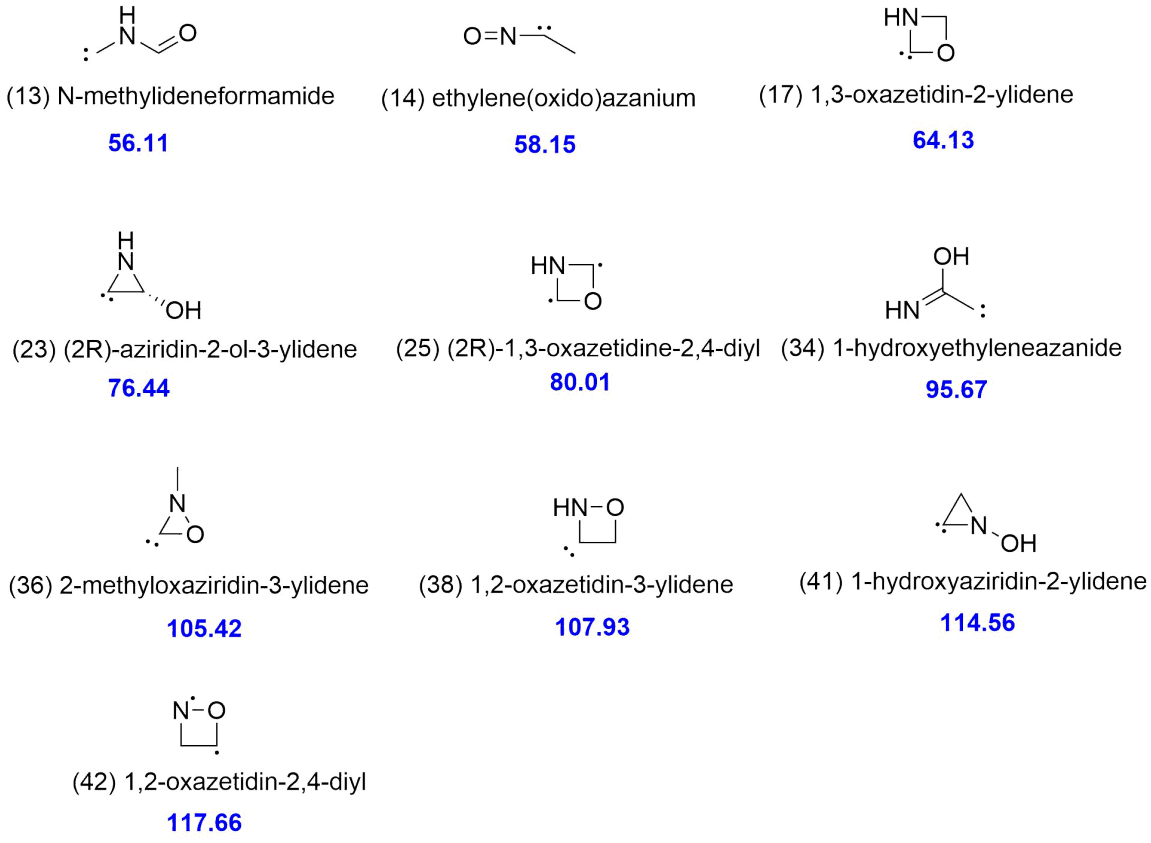

Figure 2: Diradical C_2H_3NO isomers with their IUPAC name and relative energy in kcal mol^{-1} (in blue)

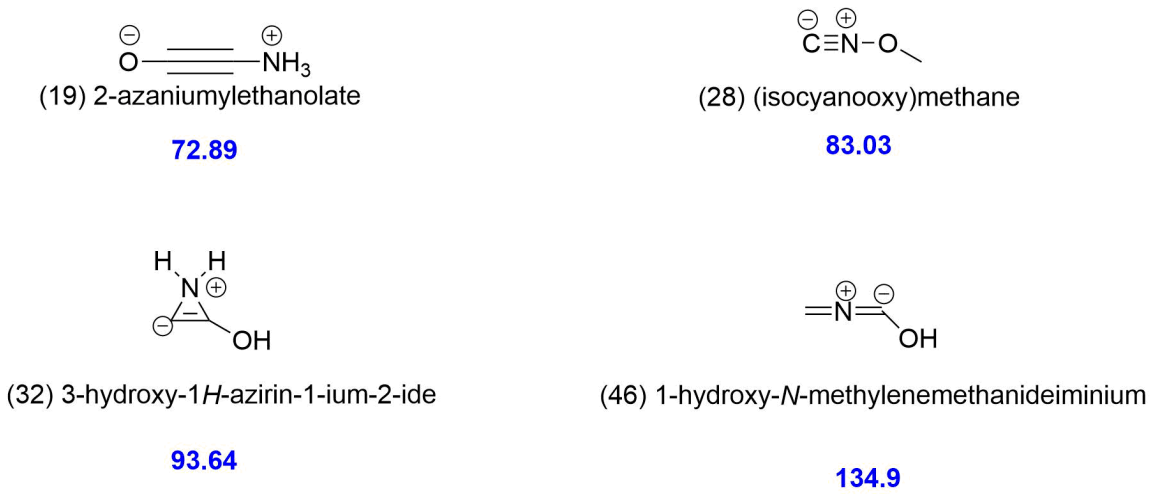

Figure 3: zwitterionic C_2H_3NO isomers with their IUPAC name and relative energy in kcal mol^{-1} (in blue)

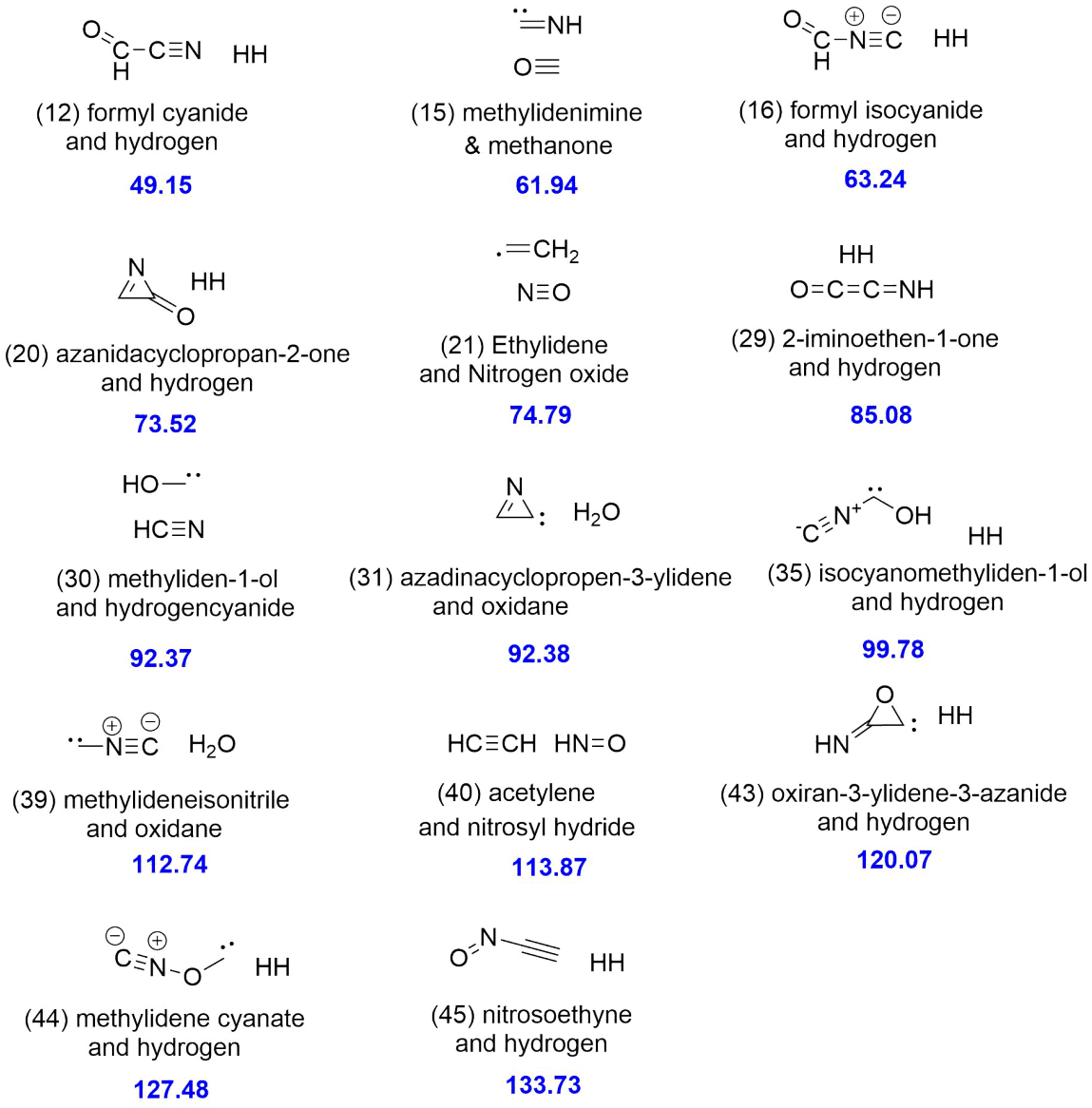

Figure 4: Dissociated C_2H_3NO isomers with their IUPAC name and relative energy in kcal mol^{-1} (in blue)

In addition to the ten most stable isomers, we found two other compounds with relative energies below 50 kcal mol^{-1}. These include 2-iminoethen-1-ol (**11**; R.E. = 43.41 kcal mol^{-1}) and formyl cyanide + hydrogen (**12**). Although compound **12** is not a C_2H_3NO isomer, we have included it and similar dissociated compounds as "byproducts" in our search for C_2H_3NO isomers. These byproducts resulted from the local optimization of randomly generated trial geometries during our investigation. Other dissociated molecular complexes are shown in Figure 4.

Alternatively, the isomers identified in our study can be classified into two main categories: acyclic and cyclic molecules, comprising 28 and 20 isomers, respectively. Acyclic isomers feature functional groups such as imine, amine, and nitrile. These isomers can be categorized into a) cyanate(**5**) and isocyanate(**1**), b) ketenimines (**11, 18, 29**) and ketene (**6**) c) imines(**3, 4, 46**) and imidic acids(**34**), d) nitriles(**2, 12, 28, 30**) and isonitrile (**16, 35, 39, 44**) , and e) ethynes (**19, 33, 40, 45, 47, 48**). Both ketenimines and imidic acids are acidic molecules, enabling them to participate in acid-base reactions. Imines exhibit nucleophilic properties, allowing them to react with electrophilic molecules. Cyanate, isocyanate, and nitriles are involved in polar reactions due to their polar nature.

a) Cyanates ($N \equiv C-O-R$) have been proposed as potential precursors of amino acids, as they can react with water to form amino acids under mild conditions.[89]

b) Isocyanates (O=C=N) are known for their reactivity and ability to participate in a wide range of chemical reactions. They have been suggested to function as intermediates in the formation of peptide bonds, which are essential for the synthesis of proteins.[90] Additionally, isocyanates have been proposed to be involved in the formation of nucleotides, the fundamental building blocks of RNA and DNA.

c) Ketenimines ($R_2C=C=NR_2$) serve as potential precursors of amino acids, as they can react with water to form amino acids under mild conditions,[91] such as in the presence of UV light. Ketenimines can tautomerize to nitrile, a prebiotic biomarker

that has been detected in extra-terrestrial regions of interest.[92] They also react with aldehydes and ketones to form α-amino acids.[93]

d) Ketene (C=C=O) are proposed as potential prebiotic precursor. The carbon-carbon double bond and carbonyl group makes it a versatile molecule that can participate in a variety of chemical reaction. It can react with ammonia to form aminoacetonitrile,[94] a precursor to amino acid like glycine.[95]

e) Nitriles (RCN) can react with water or ammonia to form α-amino nitriles, which can then be hydrolyzed to form α-amines. Nitriles can give rise to ketenimines, isonitriles, and cyanates,[96] some prebiotic precursors.

f) Isonitriles(RNC) or isocyanides can react with aldehyde and ketones to form imines,[97] which then reacts with amino acids to form peptides.

g) Imines (R_2C=NR) can react with cyanide to form α-amino nitriles, which can be hydrolyzed to form α-amino acids.[98–100]

h) Imidic acids (R_2C(=NR)OH) have been suggested as precursors of α-amino acids[101] because they can undergo decarboxylation to form ketenimines, which can then react with water or aldehydes to form amino acids.[93]

i) Ethyne (R−C≡C−R) and its derivative can react to produce amino acid.[102]

The cyclic compounds identified in our study primarily consist of 3 and 4-membered N-heterocycles and O-heterocycles. O-heterocycles, such as oximes, have been demonstrated to play a role in the synthesis of sugars, which are crucial biomolecules in living organisms. N-heterocycles, including aziridine and oxetene, may contribute to the formation of pyrimidine precursors, essential components of nucleotides found in RNA and DNA.

In our global minima search for the C_2H_3NO molecular system, we identified ten radical species with relative energies greater than 50 kcal mol^{-1} compared to the global minima. The most stable radical isomer, N-methyledineformamide (**13**), has a relative energy of 56.11 kcal mol^{-1}, followed by ethylene(oxido)azanium (**14**) at 58.15 kcal mol^{-1}. We also discovered one acyclic radical, 1-hydroxyethylenazanide (**34**), and seven cyclic radicals, including 1,3-oxazetidin-2-ylidene (**17**) and (2R)-aziridin-2-ol-3-ylidene (**23**), among others (Figure 3).

In our exploration of the C_2H_3NO molecular system, we identified four zwitterionic species with relative energies exceeding 70 kcal mol^{-1} compared to the global minima (**1**). These include three acyclic zwitterionic species: 2-azaniumylethanolate (**19**) with a relative energy of 72.89 kcal mol^{-1}, methoxy(methyl)azanide (**28**) at 83.03 kcal mol^{-1}, and 1-hydroxymethylenemethanideiminium (**46**) with relative energy of 134.9 kcal mol^{-1}. Additionally, we discovered a cyclic zwitterionic species, 3-hydroxy-1H-azirin-1-ium-2-ide (**32**), with a relative energy of 93.64 kcal mol^{-1}.

In our pool of C_2H_3NO isomers, we identified several additional dissociated molecular complexes apart from isomer **12** (R.E. = 49.15 kcal mol^{-1}) previously mentioned. We observed methylidenimine and methanone (carbon monoxide) (**15**) with an R.E. of 61.94 kcal mol^{-1}, ethylidene and nitric oxide (**21**, R.E. = 74.79 kcal mol^{-1}), methyliden-1-ol and HCN (**30**; R.E. = 112.74 kcal mol^{-1}), and nitrosyl hydride and acetylene (**40**; R.E. = 113.87 kcal mol^{-1}). In two cases, we observed water as a dissociated molecule in conjunction with azadinacyclopropen-3-ylidene (**31**; R.E. = 92.38 kcal mol^{-1}) and methylideneisonitrile (**39**; R.E. = 112.74 kcal mol^{-1}). The complexes found with hydrogen molecule include formyl isocyanide (**16**; R.E. = 63.24 kcal mol^{-1}), a cyclic molecule azanidacyclopropan-2-one (**20**; R.E. = 73.52 kcal mol^{-1}), 2-iminoethen-1-one and hydrogen (**29**; R.E. = 85.08 kcal mol^{-1}), isocyanomethyliden-1-ol (**35**; R.E. = 99.78 kcal mol^{-1}), oxiran-2-ylidene-3-azanide (**43**; R.E. = 120.07 kcal mol^{-1}), methylidenecyanate (**44**; R.E. = 127.48 kcal mol^{-1}), and an ethene derivative, nitrosoethyne (**45**; R.E. = 133.73 kcal mol^{-1}).

Some of the species obsereved in the dissociated C_2H_3NO isomers; Formyl cyanide (**12**), Methyleneisonitrile (**39**), acetylene and nitrosyl hydride (**40**), Nitrosoethyne (45) were already been detected in ISM. They have been reported due to there ability to further react and result in some building blocks of life. For example,formyl cyanide (**12**) gives glycine on reaction with water and ammonia. Nitrosoethyne (**45**) on reaction with water it can give formamide, a well known biomarker. Then on reaction with ammonia it gives cyanoacetylene, another frequently reported biomarker. Methyleneisonitrile (**39**) was found to be a precursor to glycine on reaction with water, and aminoacetonitrile when it reacts with ammonia. Acetylene formed along with nitrosyl hydride (**40**) can polymerize to polyaromatic hydrocarbons (PAHs). Reaction of acetylene with water gives ketene, a relevant precursor as discussed earlier.

In our comprehensive investigation of the C_2H_3NO isomer landscape, we have uncovered a diverse array of acyclic and cyclic molecules, radical and zwitterionic species, as well as dissociated molecular complexes. This rich chemical space, which includes several cyclic compounds, emphasizes their significance in prebiotic chemistry as potential contributors to the formation of essential biomolecules during the early stages of life.

The less stable radical and zwitterionic species offer interesting opportunities for further exploration of the C_2H_3NO system, as they may participate in various reaction pathways or serve as intermediates in the formation of more stable isomers or other critical prebiotic molecules. Their presence adds complexity and diversity to the C_2H_3NO chemical space, suggesting potential implications in prebiotic chemistry and biomolecule formation.

In the following section, we will delve deeper into the reaction space of C_2H_3NO, examining the reactions involving more fundamental building blocks, namely HCN, HNC, and HCHO.

Automated Reaction Search for C_2H_3NO

C_2H_3NO Isomers from Reaction of HCHO with HCN

Our automated exploration of the reactions between HCHO and a) HCN and b) HNC predicted five products for each reaction. On further analysis of the reaction paths for each reaction, we identified two predicted products from HCN + HCHO reaction are two-step processes. In these two cases, the first step is the isomerization of HCN to HNC. Therefore these two reactions are shown along with the HNC+HCHO reactions.

The reaction of HCHO with HCN generated N-methyleneformamide (**3**), (E)-2-iminoacetaldehyde (**4**), and 4H-1,2-oxazete (**26'**), as depicted in Figure 5. Similarly, the reaction between HCHO and HNC produced 1,3-oxazete-2-ylidene (**8'**), isocyanometanol (isoglyconitrile) (**49**), (Z)-2-iminoacetaldehyde (**4'**), oxirane-2-imine (**9**), 2-iminoethen-1-ol (**11**), and 4H-1,2-oxazet-3-ylidene (**38**), as depicted in Figure 6.

Among the nine products from these two reaction searches, five (**3, 4, 9, 11, and 38**) were also identified in our chemical space exploration. In addition, our reaction search found four other products: **26'**, **4'**, **8'**and **49**. A noteworthy product is **11**, an H-shift tautomer of gylcolonitrile (**2**). Compound **26'** is an H-shifted tautomer of **26** and is more stable than **26** by 11.36 kcal mol^{-1}. Likewise compound **8** is an H-shifted tautomer of **8'** and is more stable than **26** by 26.1 kcal mol^{-1}. The compound **4'** is the Z-conformer of **4**; **4'** is less stable than **4** by 5.6 kcal mol^{-1}. Interestingly, isocyanomethanol (49), obtained from the reaction search, was not identified in the global minima search. It has a relative energy of 31.99 kcal mol^{-1} compared to the global minimum methylimino(oxo)methane (**1**). These products highlight the complementary nature of our reaction search and global minima search approaches in uncovering a diverse range of C_2H_3NO isomers.

To gain deeper insights into the reaction mechanisms, we examined the minimum energy paths for all ten reactions, followed by a transition state (TS) search and thermochemistry analysis at 158K, a temperature representative of the hot region of IRAS 16293-

2422. Our investigation revealed that when HCHO reacts with HNC, oxirane-2-ylazanide (**9**) is the most kinetically favorable product, whereas (Z)-2-iminoacetaldehyde (**4′**) is the thermodynamically most feasible product. On the other hand, when HCHO reacts with HCN, N-methyleneformamide (**3**) emerges as the most thermodynamically and kinetically controlled product. In the following sections, we provide a detailed analysis of each reaction.

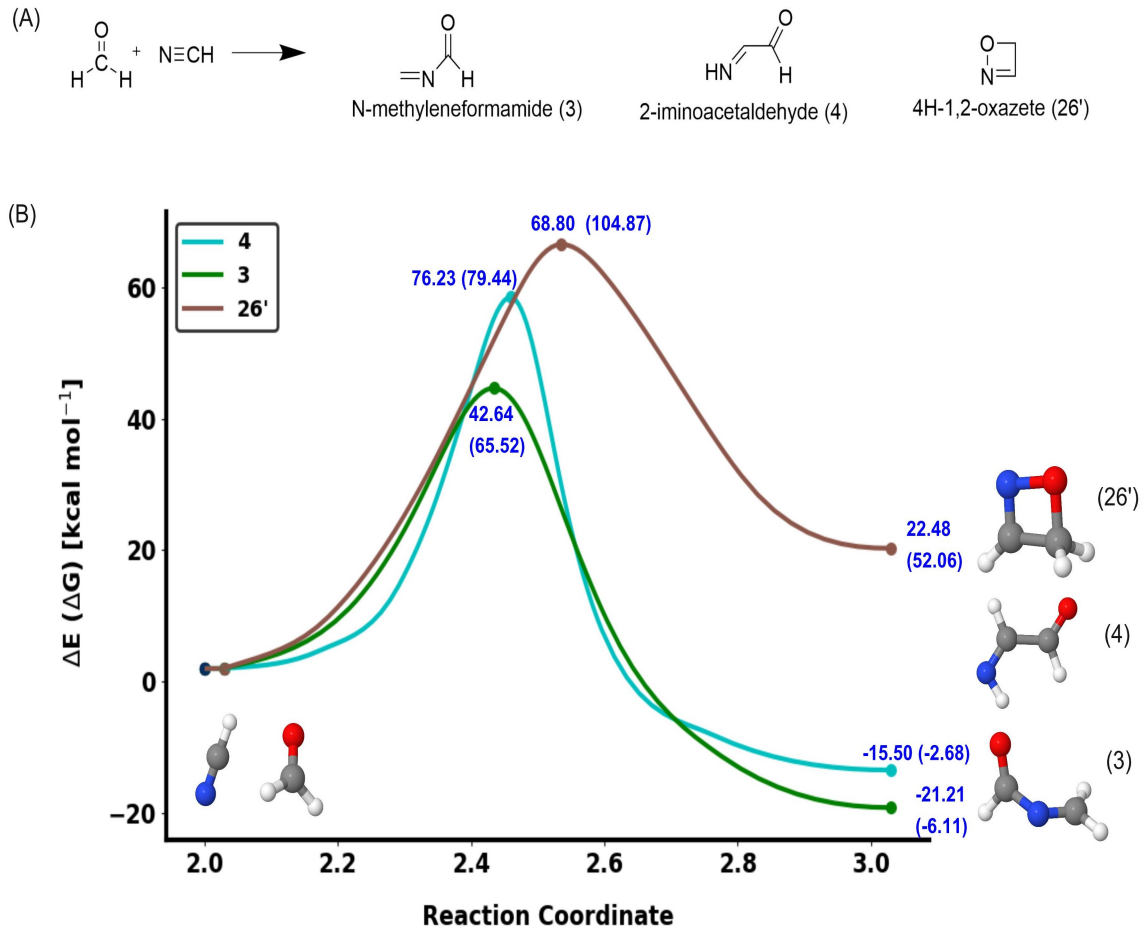

Figure 5: A) Products obtained through the automated reaction search involving HCN and HCHO. B) Electronic energy profiles derived from nudged elastic band calculations for pathways to 3, 4, and 26′. The Gibbs free energy of the TS relative to the reactant complexes is shown in parentheses.

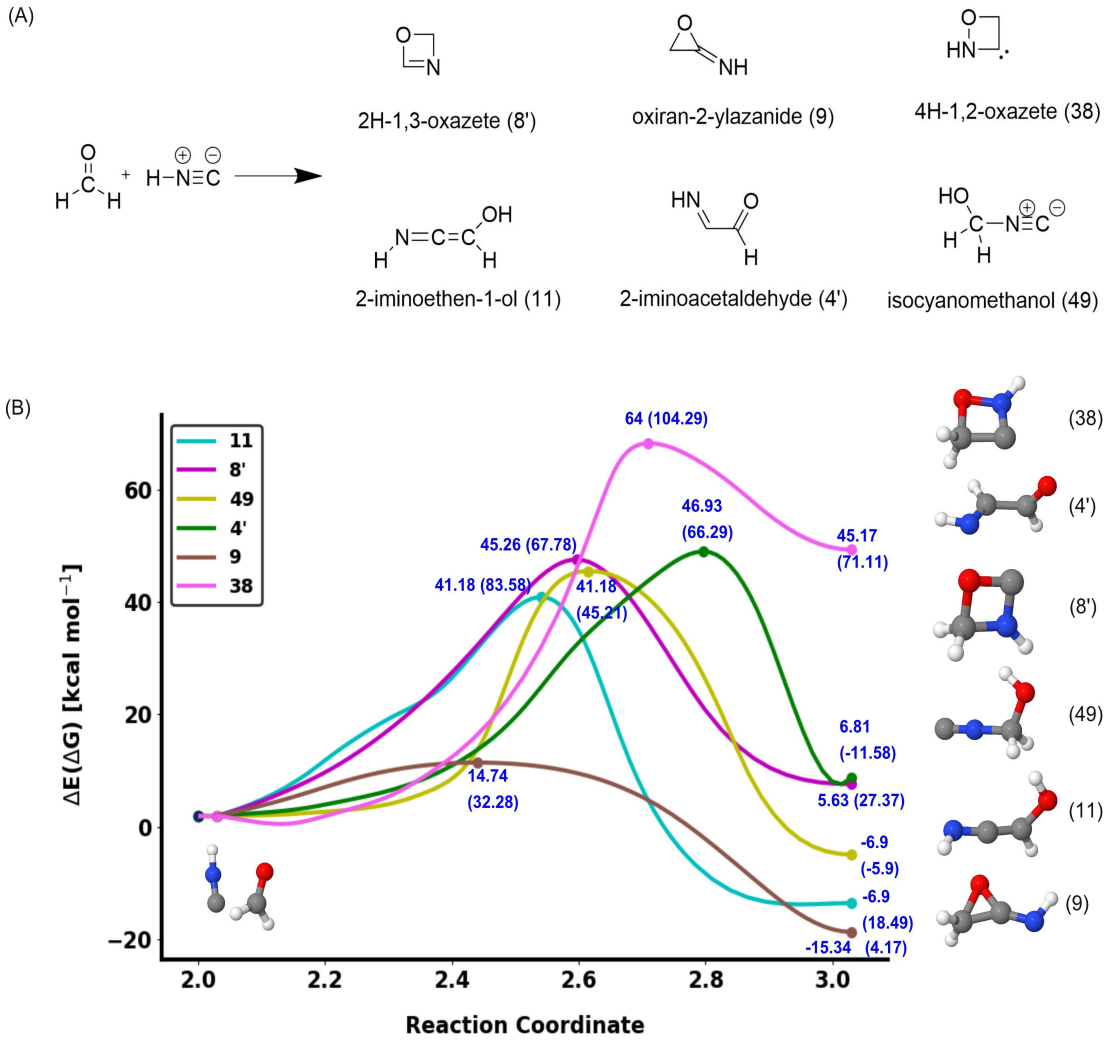

Figure 6: A) Products obtained through the automated reaction search involving HCN and HCHO. B) Electronic energy profiles derived from nudged elastic band calculations for pathways **8′, 9, 11, 38, 4′**, and **49**. The Gibbs free energy of the TS relative to the reactant complexes is shown in parentheses.

Reaction Mechanisms of the product formation

1. **2-Iminoethen-1-ol (11):** The formation of 2-iminoethen-1-ol (11) from HCN and HCHO involves a C-C bond formation between the reactants, followed by an H-shift from C to O. This process results in an increase in the C-O bond length from 1.21 Å to 1.39 Å. The reaction requires an activation barrier ($\Delta G^{\ddagger}$) of 83.58 kcal mol^{-1}, and has a free energy change of 18.49 kcal mol^{-1}.

2. **Isoglyconitrile (49):** Isocyanomethanol (49), also known as isoglyconitrile, is observed in the reaction search between HNC and HCHO. In this reaction, the hydrogen atom from HNC transfers to the oxygen atom of HCHO, yielding NC^{-} and $HCHOH^{+}$, followed by a N-C bond formation with a bond length of 1.42 Å. The formation of 49 proceeds via an exothermic pathway, characterized by a free energy change of -11.58 kcal mol^{-1} and an activation energy of 66.29 kcal mol^{-1}.

3. **(E)-2-iminoacetaldehyde (4) and (Z)-2-iminoacetaldehyde (4'):** (E)-2-iminoacetaldehyde (**4)** forms from HCHO and HCN through a hydrogen transfer from HCHO to the nitrogen of HCN, followed by the formation of a new C-C bond (1.50 Å) between the reactants. This reaction has an activation energy of ($\Delta G^{\ddagger}$) 79.44 kcal mol^{-1} and is exothermic, with a reaction energy of (ΔG) -2.68 kcal mol^{-1}. Similarly, the reaction between HNC and HCHO generates the Z-isomer, (Z)-2-iminoacetaldehyde (**4**), by a hydrogen transfer from HCHO to the carbon of HNC, followed by the formation of a C-C bond (1.69 Å) between the reactants. This reaction has an activation energy ($\Delta G^{\ddagger}$) of 66.29 kcal mol^{-1} and a reaction energy of (ΔG) -11.58 kcal mol^{-1}. Both iminoacetaldehydes form via exothermic pathways, with **4'** being thermodynamically more stable.

4. **N-methyleneformamide (3):** The thermodynamically most favorable pathway from the HCN and HCHO reaction results in the formation of N-methyleneformamide (**3**). The CONH moiety in 3 can potentially act as a peptide linkage, leading to a

nucleoside chain upon further reaction. In this product, a new C-N bond (1.402 Å) is formed between the carbon of HCHO and the nitrogen of HCN, accompanied by a simultaneous hydrogen transfer from the carbon of HCHO to the carbon of HCN. The minimum energy path of the reaction surmounts an activation barrier ($\Delta G^{\ddagger}$) of 65.52 kcal mol^{-1}, and the reaction energy is (ΔG) -6.11 kcal mol^{-1}, as illustrated in Figure 6.

5. **oxiran-2-ylazanide (9) :** The formation of oxirane-2-ylazanide from the reaction between HNC and HCHO follows a slightly endothermic pathway, exhibiting a reaction energy of 4.17 kcal mol^{-1}. In this reaction, the carbon atom of HNC simultaneously forms bonds with the carbon and oxygen atoms of HCHO, resulting in a three-membered heterocyclic ring. The C=O bond in the HCHO moiety increases from 1.2 Å to 1.5 Å, while new C-O and C-C bonds form, with lengths of 1.35 Å and 1.45 Å, respectively. The reaction has an activation energy barrier ($\Delta G^{\ddagger}$) of 36.28 kcal mol^{-1}.

6. **4H-1,2-oxazete (26')** The four-membered heterocyclic compound, 4H-1,2-oxazete (**26'**), is formed endothermically (ΔG = 52.06 kcal mol^{-1}) through a [2+2] cycloaddition reaction between HCN and HCHO. In this process, the C=O bond length changes from 1.2 Å to 1.47 Å, and the C≡N bond length changes from 1.15 Å to 1.3 Å, resulting in the formation of **26'**. The activation energy barrier is very high ($\Delta G^{\ddagger}$ = 104.87 kcal mol^{-1}).

7. **1,2-oxazete-3-ylidene (38)** The diradical species, 1,2-oxazete-3-ylidene (**38**), is formed from the reaction between HNC and HCHO through a [2+2] cycloaddition process. This reaction is highly endothermic, as indicated by the reaction energy (ΔG) of 71.11 kcal $^{-1}$. The activation energy barrier ($\Delta G^{\ddagger}$) required for this reaction is 104.29 kcal $^{-1}$. In the formation of **38**, the C=O bond length changes from 1.21 Å to 1.52 Å and the C ≡ N bond length from 1.17 Å to 1.3 Å.

8. **1,3-oxazete-2-ylidene (8′)** The endothermic formation of 1,3-oxazete-2-ylidene (**8′**) occurs through a [2+2] cycloaddition reaction between HNC and HCHO, with a reaction energy (ΔG) of 27.37 kcal mol^{-1}. The activation energy barrier ($\Delta G^{\ddagger}$) for this reaction is 67.78 kcal mol^{-1}. During the reaction, the C=O bond length changes from 1.2 Å to 1.45 Å, and the C≡N bond length shifts from 1.17 Å to 1.36 Å.

The comprehensive investigation of the reaction mechanisms and pathways in this study has provided valuable insights into the formation of various C_2H_3NO isomers from HCHO and HCN/HNC reactions. Our findings highlight the importance of both kinetically and thermodynamically controlled products, such as oxirane-2-ylazanide (**9**) and (Z)-2-iminoacetaldehyde (**4′**), in understanding the complex processes that govern the formation of these isomers. In the upcoming section, we will further evaluate the kinetic stability of these C_2H_3NO isomers by employing ADMP (Atom-centered Density Matrix Propagation) simulations. These simulations will provide a more detailed understanding of the dynamic behavior of these molecules and their stability under various conditions.

Kinetic Stability of Products Obtained from Reactions

To investigate the kinetic stability of the C_2H_3NO isomers identified in this study, ADMP simulations were carried out at various temperatures. The time evolution of total energies from the ADMP simulation (refer to Methods for details) at 158K, illustrated by snapshots at 2,000 fs intervals, shows the geometric changes occurring in each molecule over a 10,000 fs period. These results are provided in Supporting Information Figures S1 to S9. Throughout the duration, the figures display stable energy oscillations and minimal geometric alterations, indicating that these molecules are kinetically stable. These findings of kinetic stability in the simulations suggest that these C_2H_3NO isomers can act as stable intermediates in forming essential biomolecules in prebiotic pathways under various conditions.

Rotational Analysis

The spectral properties of C_2H_3NO isomers were calculated to provide theoretical data for further investigation of the products formed. Detecting these products could indicate the presence of HCHO and HCN in the medium, enabling more in-depth studies of reactions involving these biomarkers. Rotational constants, A_e, B_e, C_e (equilibrium rotational constants), and A_o, B_o, C_o (vibrationally corrected rotational constants) are provided for the isomers obtained from global optimization (1-48), as well as for **4′, 8′, 26′**, and **49** in Tables 1-3. We have also provided quartic and sextic distortion constants for the isomers obtained from HCN/HNC and HCHO reactions, specifically for species **3, 4, 9, 11, 38, 8′, 4′, 26′**, and **39**, in S5-S12.

All the identified isomers possess non-zero dipole moments, rendering them rotationally active. Each molecular species displays C1 symmetry and has three distinct moments of inertia along mutually orthogonal axes, with the center of mass as the origin. As a result, each species exhibits three independent rotational constants (Ae, Be, and C_e), characterizing them as asymmetric top molecules. Ray's asymmetric parameter, κ, quantitatively represents the deviation of a molecule from symmetry. The acyclic isomers obtained in our study can be classified as 'near-prolate' type asymmetric tops based on their κ values, ranging from -0.90 to -0.99. Similarly, the species with κ values ranging from 0.90 to 0.99 are categorized as 'near-oblate' type asymmetric tops. Our results reveal that oxirane-2-ylazanide is a prolate asymmetric top with a κ value of -0.831 and an equilibrium rotational constant (A_e) significantly larger than B_e and C_e constants, indicating the molecule's highly prolate shape. Other 3-membered N-heterocyclic compounds have κ values between -0.700 and -0.991. In contrast, the 4-membered N-heterocyclic oxazete belongs to the oblate asymmetric top category, with κ values ranging from 0.534 to 0.903. The equilibrium rotational constants for this molecule reveal that A_e and B_e are similar in magnitude but much larger than C_e, indicating a flattened, oblate shape for the molecule.

Table 1: Rotational parameters for C_2H_3NO isomers computed with uwb97xd/6-311++G(2D,2P) level of theory. κ is ray's asymmetric parameter. A_e, B_e, C_e are the equilibrium rotational constants. A_o, B_o, C_o are the vibrationally corrected rotational constants.

Species	κ	A_e	B_e	C_e	A_o	B_o	C_o
1	-0.996741	78622.536	4399.242	4278.11	82114.392	4359.058	4253.63
2	-0.970145	34238.866	4849.051	4403.687	34098.286	4834.606	4383.49
3	-0.937863	29779.874	6164.782	5407.573	30453.784	6038.636	5341.873
4	-0.984271	53910.444	4780.955	4391.503	53287.091	4757.654	4368.68
5	-0.973164	40334.955	5330.481	4854.41	40233.139	5303.228	4824.79
6	-0.983042	44691.931	4662.787	4320.483	44986.498	4638.466	4295.654
7	-0.806465	23327.546	7869.726	6213.657	23091.097	7842.07	6171.19
8	0.63267	16306.154	14813.296	8177.989	16170.004	14701.259	8106.674
9	-0.831834	25204.438	7812.68	6216.082	24959.271	7778.878	6174.624
10	-0.835772	24674.497	7545.779	6013.446	24376.718	7518.969	5974.649
11	-0.985724	46943.028	4574.689	4270.082	47221.228	4553.835	4245.604
12	-0.989038	68084.976	5040.444	4693.013	68647.629	5025.364	4675.59
13	-0.980965	52748.904	5146.042	4688.632	52046.784	5113.406	4656.578
14	-1.000000	160255.464	3938.455	3938.452	158295.648	3935.446	3935.455
15	-0.9698359	244846.255	30069.313	26780.444	248105.081	29939.869	26401.761
16	-0.978684	54824.065	5698.99	5169.797	56480.944	5673.726	5136.021
17	0.583743	16398.798	14683.578	8157.64	16270.087	14542.999	8090.553
18	-0.988701	51248.531	4717.647	4453.272	50680.48	4708.763	4437.353
19	-0.991338	56182.449	4380.764	4155.426	55496.612	4372.376	4149.368
20	-0.913758	39054.896	8109.976	6715.47	38877.024	8076.836	6677.557
21	-0.881968	26407.332	6415.194	5161.338	26337.164	6367.191	5120.701
22	-0.700921	19775.228	7961.251	5883.958	19691.392	7925.897	5849.54
23	-0.934502	24864.38	7394.393	6802.895	24678.614	7350.391	6756.565
24	-0.7937	23949.338	7914.581	6070.362	23737.58	7887.716	6033.735
25	0.612061	16947.41	15250.436	8198.742	17041.974	15322.186	8202.685
26	0.903033	15687.298	15310.637	7918.396	15567.095	15198.99	7850.725
27	-0.859881	24521.898	7630.608	6358.063	24353.487	7573.298	6299.767
28	-0.966234	38665.696	5686.608	5120.255	38581.149	5655.464	5086.409
29	-0.960116	28957.973	4089.358	3583.331	12228.34	4341.102	3507.981
30	-0.9844304	376002.529	33175.243	30485.468	381209.843	33065.392	30072.5
31	-0.991666	37391.289	2413.691	2267.334	38862.952	2397.224	2247.067
32	-0.628533	18570.074	8268.352	5918.537	18026.697	8298.235	5871.069
33	-0.967625	37889.429	5317.587	4781.651	38078.36	5278.645	4744.995
34	-0.103483	14405.195	9748.788	5965.719	14475.14	9653.531	5927.645
35	-0.978919	43400.339	4455.738	4040.877	58707.579	4238.393	3988.914

Rotational parameters for C_2H_3NO isomers computed with uwb97xd/6-311++G(2D,2P) level of theory. κ is ray's asymmetric parameter. A_e, B_e, C_e are the equilibrium rotational constants. A_o, B_o, C_o are the vibrationally corrected rotational constants.

Species	kappa	A_e	B_e	C_e	A_o	B_o	C_o
36	-0.929291	24963.688	7663.187	7029.115	24839.488	7590.345	6963.17
37	-0.889048	22592.536	7891.791	7028.355	22458.822	7820.115	6962.388
38	0.724976	15662.511	14601.458	7946.434	15541.219	14474.288	7875.776
39a	-0.998808	513373.422	12532.353	12233.752	508962.635	12519.479	12210.905
39b	-0.461408	836352.79	434014.584	285735.698	851115.407	431634.821	279028.978
40	-0.973535	25280.694	2908.098	2608.084	48776.115	1820.767	1975.495
41	-0.803574	23554.522	7841.372	6130.06	23328.89	7785.926	6082.698
42	0.584523	16162.326	14472.691	8028.857	16053.761	14369.275	7968.98
43	-0.909994	38539.788	8175.764	6744.915	38421.666	8125.506	6696.659
44	-0.985214	61071.792	5719.285	5307.006	61081.094	5718.558	5289.232
45	-0.989085	68210.72	5039.057	4692.408	68784.666	5024.001	4675.025
46	-0.991567	57941.244	4799.185	4574.169	61661.525	4710.622	4484.351
47	-0.782006	21661.809	7151.583	5376.536	21350.107	7173.001	5371.278
48	-0.943237	2.973	0.598	0.528	2.973	0.598	0.528

Table 2: Rotational parameters A_e, B_e, C_e (equilibrium rotational constants), and A_o, B_o, C_o (vibrationally corrected rotational constants). κ and μ (in Debye) of the isomers computed with uwb97xd/6-311++G for C_2H_3NO isomers formed upon HCN and HCHO reaction apart from global minima search.

Isomers	κ	μ	A_e	B_e	C_e	A_o	B_o	C_o
26′	0.534570	3.62	15997.127	14107.413	7876.841	15871.088	13999.681	7809.669
8′	0.583973	4.73	16400.380	14686.033	8158.850	16271.300	14546.245	8091.594
4′	-0.892985	4.11	26217.836	6064.623	4925.315	26428.445	5957.283	4895.898
49	-0.966457	3.10	34612.662	5233.751	4732.622	34469.226	5220.784	4711.524

Conclusion

In this study, we aim to understand better the chemical processes that led to the formation of life on Earth and elsewhere in the universe by exploring the chemical and reaction space of C_2H_3NO isomers, including well-known biomarkers such as formyl cyanide, nitrosoethyne, methyleneisonitrile, acetylene, glycolonitrile, and N-methyleneformamide. Using global optimization coupled with density functional theory (DFT)-based calculations, we explore the potential energy surface (PES) of C_3H_2NO isomers, encompassing a diverse landscape of acyclic and cyclic molecules, radical and zwitterionic species, as well as dissociated molecular complexes. Additionally, we studied the bimolecular reactions of HCN and HNC with H_2CO using an artificial force-induced reaction-based automated search and transition state search to identify the minimal energy routes. This generated products, some already found through the global minima search, while we also discovered new molecules, (Z)2-iminoacytaldehyde, 4H-1,2-oxazete, and isocyanomethanol. We provided detailed analyses of each reaction and calculated their activation energies from the located transition states. To confirm the kinetic stability of the molecules, we employ atomistic molecular dynamics simulations. Finally, we present computed rotovibrational spectral parameters to aid in the future detection of these molecules in the interstellar medium. Overall, our study sheds light on the chemical space of C_2H_3NO isomers and their potential role in the emergence of life in the universe.

Acknowledgement

We acknowledge the National Supercomputing Mission (NSM) for providing computing resources of 'PARAM Shakti' at IIT Kharagpur, which is implemented by C-DAC and supported by the Ministry of Electronics and Information Technology (MeitY) and Department of Science and Technology (DST), Government of India.

References

(1) Hazen, R. M. Paleomineralogy of the Hadean Eon: A preliminary species list. *American Journal of Science* **2013**, *313*, 807–843.

(2) Gargaud, M. *Lectures in Astrobiology: Vol I: Part 2: From Prebiotic Chemistry to the Origin of Life on Earth*; Springer Science & Business Media, 2006.

(3) Kolb, V. M. *Astrobiology: an evolutionary approach*; CRC Press, 2014.

(4) Cottin, H.; Kotler, J. M.; Bartik, K.; Cleaves, H. J.; Cockell, C. S.; De Vera, J.-P. P.; Ehrenfreund, P.; Leuko, S.; Ten Kate, I. L.; Martins, Z., et al. Astrobiology and the possibility of life on earth and elsewhere.... *Space Science Reviews* **2017**, *209*, 1–42.

(5) Knoll, A. H.; Carr, M.; Clark, B.; Des Marais, D. J.; Farmer, J. D.; Fischer, W. W.; Grotzinger, J. P.; McLennan, S. M.; Malin, M.; Schröder, C., et al. An astrobiological perspective on Meridiani Planum. *Earth and Planetary Science Letters* **2005**, *240*, 179–189.

(6) Des Marais, D. J.; Allamandola, L. J.; Benner, S. A.; Boss, A. P.; Deamer, D.; Falkowski, P. G.; Farmer, J. D.; Hedges, S. B.; Jakosky, B. M.; Knoll, A. H., et al. The NASA astrobiology roadmap. *Astrobiology* **2003**, *3*, 219–235.

(7) De Mol, M. L. Astrobiology in Space: A Comprehensive Look at the Solar System. *Life* **2023**, *13*, 675.

(8) Ferris, J. P.; Hagan Jr, W. J. HCN and chemical evolution: the possible role of cyano compounds in prebiotic synthesis. *Tetrahedron* **1984**, *40*, 1093–1120.

(9) BOK, B. J. The Planets: Their Origin and Development. Harold C. Urey. New Haven, Conn.: Yale Univ. Press, 1952. 245 pp. 5.00. *Science* **1952**, *115*, 689–690.

(10) Green, N. J.; Xu, J.; Sutherland, J. D. Illuminating life's origins: UV photochemistry in abiotic synthesis of biomolecules. *Journal of the American Chemical Society* **2021**, *143*, 7219–7236.

(11) Krishnamurthy, R. Life's biological chemistry: a destiny or destination starting from prebiotic chemistry? *Chemistry–A European Journal* **2018**, *24*, 16708–16715.

(12) Rode, B. M. Peptides and the origin of life1. *Peptides* **1999**, *20*, 773–786.

(13) Lazcano, A.; Bada, J. L. The 1953 Stanley L. Miller experiment: fifty years of prebiotic organic chemistry. *Origins of Life and Evolution of the Biosphere* **2003**, *33*, 235–242.

(14) Ehrenfreund, P.; Irvine, W.; Becker, L.; Blank, J.; Brucato, J.; Colangeli, L.; Derenne, S.; Despois, D.; Dutrey, A.; Fraaije, H., et al. Astrophysical and astrochemical insights into the origin of life. *Reports on progress in physics* **2002**, *65*, 1427.

(15) Ehrenfreund, P.; Spaans, M.; Holm, N. G. The evolution of organic matter in space. *Philosophical Transactions of the Royal Society A: Mathematical, Physical and Engineering Sciences* **2011**, *369*, 538–554.

(16) Fulvio, D.; Potapov, A.; He, J.; Henning, T. Astrochemical pathways to complex organic and prebiotic molecules: Experimental perspectives for in situ solid-state studies. *Life* **2021**, *11*, 568.

(17) Sandford, S. A.; Nuevo, M.; Bera, P. P.; Lee, T. J. Prebiotic astrochemistry and the formation of molecules of astrobiological interest in interstellar clouds and protostellar disks. *Chemical reviews* **2020**, *120*, 4616–4659.

(18) Boogert, A. A.; Gerakines, P. A.; Whittet, D. C. Observations of the icy universe. *Annual Review of Astronomy and Astrophysics* **2015**, *53*, 541–581.

(19) Snow, T. P. Ultraviolet observations of interstellar molecules. *Proceedings of the International Astronomical Union* **2005**, *1*, 175–186.

(20) Weaver, H.; Mumma, M. Infrared molecular emissions from comets. *Astrophysical Journal, Part 1 (ISSN 0004-637X), vol. 276, Jan. 15, 1984, p. 782-797.* **1984**, *276*, 782–797.

(21) Karska, A.; Herpin, F.; Bruderer, S.; Goicoechea, J.; Herczeg, G.; Van Dishoeck, E.; San José-García, I.; Contursi, A.; Feuchtgruber, H.; Fedele, D., et al. Far-infrared molecular lines from low-to high-mass star forming regions observed with Herschel. *Astronomy & Astrophysics* **2014**, *562*, A45.

(22) Barone, V.; Biczysko, M.; Puzzarini, C. Quantum chemistry meets spectroscopy for astrochemistry: Increasing complexity toward prebiotic molecules. *Accounts of chemical research* **2015**, *48*, 1413–1422.

(23) Rivière, A.; Eeltink, S.; Pierlot, C.; Balzarini, T.; Moens, F.; Selak, M.; De Vuyst, L. Development of an ion-exchange chromatography method for monitoring the degradation of prebiotic arabinoxylan-oligosaccharides in a complex fermentation medium. *Analytical chemistry* **2013**, *85*, 4982–4990.

(24) Öberg, K. I. Photochemistry and astrochemistry: Photochemical pathways to interstellar complex organic molecules. *Chemical reviews* **2016**, *116*, 9631–9663.

(25) Pérez-Villa, A.; Pietrucci, F.; Saitta, A. M. Prebiotic chemistry and origins of life

research with atomistic computer simulations. *Physics of life reviews* **2020**, *34*, 105–135.

(26) Schwartz, A. W.; Goverde, M. Acceleration of HCN oligomerization by formaldehyde and related compounds: Implications renderix-prebiotic-afcf9d716623.zipa tentative mechanism is suggested, significantly extend the possible range of conditions for HCN oligomerization on the prebiotic Earth. *Journal of Molecular Evolution* **1982**, 351–353.

(27) Koch, D. M.; Toubin, C.; Peslherbe, G. H.; Hynes, J. T. A theoretical study of the formation of the aminoacetonitrile precursor of glycine on icy grain mantles in the interstellar medium. *The Journal of Physical Chemistry C* **2008**, *112*, 2972–2980.

(28) Schwartz, A. W.; Joosten, H.; Voet, A. Prebiotic adenine synthesis via HCN oligomerization in ice. *Biosystems* **1982**, *15*, 191–193.

(29) Zhao, G.; Quan, D.; Zhang, X.; Feng, G.; Zhou, J.; Li, D.; Meng, Q.; Chang, Q.; Yang, X.; He, M., et al. Glycolonitrile (HOCH2CN) Chemistry in Star-forming Regions. *The Astrophysical Journal Supplement Series* **2021**, *257*, 26.

(30) Halfen, D.; Ilyushin, V.; Ziurys, L. Formation of peptide bonds in space: a comprehensive study of formamide and acetamide in Sgr B2 (N). *The Astrophysical Journal* **2011**, *743*, 60.

(31) Hollis, J.; Lovas, F. J.; Remijan, A. J.; Jewell, P.; Ilyushin, V. V.; Kleiner, I. Detection of acetamide (CH3CONH2): The largest interstellar molecule with a peptide bond. *The Astrophysical Journal* **2006**, *643*, L25.

(32) Frigge, R.; Zhu, C.; Turner, A. M.; Abplanalp, M. J.; Bergantini, A.; Sun, B.-J.; Chen, Y.-L.; Chang, A. H.; Kaiser, R. I. A vacuum ultraviolet photoionization study on the formation of N-methyl formamide (HCONHCH3) in deep space: A potential interstellar molecule with a peptide bond. *The Astrophysical Journal* **2018**, *862*, 84.

(33) Ellinger, Y.; Pauzat, F.; Markovits, A.; Allaire, A.; Guillemin, J.-C. The quest of chirality in the interstellar medium-I. Lessons of propylene oxide detection. *Astronomy & Astrophysics* **2020**, *633*, A49.

(34) Vrtilek, J.; Gottlieb, C.; Thaddeus, P. Laboratory and astronomical spectroscopy of C3H2, the first interstellar organic ring. *The Astrophysical Journal* **1987**, *314*, 716–725.

(35) Barnum, T. J.; Lee, K. L. K.; McGuire, B. A. Chirped-Pulse Fourier Transform Millimeter-Wave Spectroscopy of Furan, Isotopologues, and Vibrational Excited States. *ACS Earth and Space Chemistry* **2021**, *5*, 2986–2994.

(36) Etim, E.; Asuquo, J.; Ngana, O.; Ogofotha, G. INVESTIGATION ON THE THERMOCHEMISTRY, MOLECULAR SPECTROSCOPY AND STRUCTURAL PARAMETERS OF PYRROLE AND ITS ISOMERS: A QUANTUM CHEMISTRY APPROACH. *Journal of Chemical Society of Nigeria* **2022**, *47*.

(37) Simmie, J. M. C2H5NO Isomers: From Acetamide to 1, 2-Oxazetidine and Beyond. *The Journal of Physical Chemistry A* **2022**, *126*, 924–939.

(38) Hehre, W. J. *A guide to molecular mechanics and quantum chemical calculations*; Wavefunction Irvine, CA, 2003; Vol. 2.

(39) Shao, Y.; Molnar, L. F.; Jung, Y.; Kussmann, J.; Ochsenfeld, C.; Brown, S. T.; Gilbert, A. T.; Slipchenko, L. V.; Levchenko, S. V.; O'Neill, D. P., et al. Advances in methods and algorithms in a modern quantum chemistry program package. *Physical Chemistry Chemical Physics* **2006**, *8*, 3172–3191.

(40) Fogel, D. B. Introduction to evolutionary computation. *Evolutionary computation* **2000**, *1*.

(41) Michalewicz, Z. Genetic algorithms, numerical optimization, and constraints. Pro-

ceedings of the sixth international conference on genetic algorithms. 1995; pp 151–158.

(42) PARTRIDGE, D. A review of:"Handbook of Genetic Algorithms" L. Davis (Ed.) New York: Van Nostrand Reinhold, 1991 ISBN 0-442-00173-8, 385pp.,£ 32.50. *Connection Science* **1991**, *3*, 446–448.

(43) Goldberg, D. E. Genetic algorithms in search, optimization and machine learning Addison Welssey Publishing company. *Reading, MA* **1989**,

(44) Wales, D. J.; Doye, J. P. Global optimization by basin-hopping and the lowest energy structures of Lennard-Jones clusters containing up to 110 atoms. *The Journal of Physical Chemistry A* **1997**, *101*, 5111–5116.

(45) Iwamatsu, M.; Okabe, Y. Basin hopping with occasional jumping. *Chemical Physics Letters* **2004**, *399*, 396–400.

(46) Zhan, L.; Chen, J. Z.; Liu, W.-K. Monte Carlo basin paving: an improved global optimization method. *Physical Review E* **2006**, *73*, 015701.

(47) Shanker, S.; Bandyopadhyay, P. Monte Carlo temperature basin paving with effective fragment potential: An efficient and fast method for finding low-energy structures of water clusters (H2O) 20 and (H2O) 25. *The Journal of Physical Chemistry A* **2011**, *115*, 11866–11875.

(48) Shoji, M.; Watanabe, N.; Hori, Y.; Furuya, K.; Umemura, M.; Boero, M.; Shigeta, Y. Comprehensive search of stable isomers of alanine and alanine precursors in prebiotic syntheses. *Astrobiology* **2022**, *22*, 1129–1142.

(49) Wang, L.-P.; Titov, A.; McGibbon, R.; Liu, F.; Pande, V. S.; Martínez, T. J. Discovering chemistry with an ab initio nanoreactor. *Nature Chemistry* **2014**, *6*, 1044–1048.

(50) Das, T.; Ghule, S.; Vanka, K. Insights Into the Origin of Life: Did It Begin from HCN and H2O? *ACS Central Science* **2019**, *5*, 1532–1540.

(51) Dash, S. R.; Das, T.; Vanka, K. Insights Into Chemical Reactions at the Beginning of the Universe: From HeH^+ to $H3^+$. *Frontiers in Chemistry* **2021**, *9*.

(52) Stan, A.; von der Esch, B.; Ochsenfeld, C. Fully Automated Generation of Prebiotically Relevant Reaction Networks from Optimized Nanoreactor Simulations. *Journal of Chemical Theory and Computation* **2022**, *18*, 6700–6712.

(53) Maeda, S.; Morokuma, K. Finding Reaction Pathways of Type A + B $\rightarrow$ X: Toward Systematic Prediction of Reaction Mechanisms. *Journal of Chemical Theory and Computation* **2011**, *7*, 2335–2345.

(54) Nandi, S.; Bhattacharyya, D.; Anoop, A. Prebiotic Chemistry of HCN Tetramerization by Automated Reaction Search. *Chemistry - A European Journal* **2018**, *24*, 4885–4894.

(55) Komatsu, Y.; Suzuki, T. Quantum Chemical Study on Interstellar Synthesis of Cytosine by the Automated Reaction Path Search. *ACS Earth and Space Chemistry* **2022**, *6*, 2491–2498.

(56) Zhang, J.; Dolg, M. ABCluster: the artificial bee colony algorithm for cluster global optimization. *Physical Chemistry Chemical Physics* **2015**, *17*, 24173–24181.

(57) Zhang, J.; Dolg, M. Global optimization of clusters of rigid molecules using the artificial bee colony algorithm. *Physical Chemistry Chemical Physics* **2016**, *18*, 3003–3010.

(58) Frisch, M.; Trucks, G.; Schlegel, H.; Scuseria, G.; Robb, M.; Cheeseman, J.; Scalmani, G.; Barone, V.; Petersson, G.; Nakatsuji, H., et al. Gaussian 16 Revision C. 01. 2016; Gaussian Inc. *Wallingford CT* **2016**, *421*.

(59) Becke, A. D. Density-functional thermochemistry. V. Systematic optimization of exchange-correlation functionals. *The Journal of Chemical Physics* **1997**, *107*, 8554–8560.

(60) Adamo, C.; Barone, V. Toward reliable density functional methods without adjustable parameters: The PBE0 model. *The Journal of chemical physics* **1999**, *110*, 6158–6170.

(61) Weigend, F.; Ahlrichs, R. Balanced basis sets of split valence, triple zeta valence and quadruple zeta valence quality for H to Rn: Design and assessment of accuracy. *Physical Chemistry Chemical Physics* **2005**, *7*, 3297–3305.

(62) Becke, A. D.; Johnson, E. R. Exchange-hole dipole moment and the dispersion interaction. *The Journal of chemical physics* **2005**, *122*, 154104.

(63) Grimme, S.; Ehrlich, S.; Goerigk, L. Effect of the damping function in dispersion corrected density functional theory. *Journal of computational chemistry* **2011**, *32*, 1456–1465.

(64) Grimme, S.; Antony, J.; Ehrlich, S.; Krieg, H. A consistent and accurate ab initio parametrization of density functional dispersion correction (DFT-D) for the 94 elements H-Pu. *The Journal of chemical physics* **2010**, *132*, 154104.

(65) Kossmann, S.; Neese, F. Efficient structure optimization with second-order many-body perturbation theory: The RIJCOSX-MP2 method. *Journal of chemical theory and computation* **2010**, *6*, 2325–2338.

(66) Zhao, Y.; Truhlar, D. G. A new local density functional for main-group thermochemistry, transition metal bonding, thermochemical kinetics, and noncovalent interactions. *The Journal of chemical physics* **2006**, *125*, 194101.

(67) Zhao, Y.; Truhlar, D. G. The M06 suite of density functionals for main group thermochemistry, thermochemical kinetics, noncovalent interactions, excited states, and transition elements: two new functionals and systematic testing of four M06-class functionals and 12 other functionals. *Theoretical chemistry accounts* **2008**, *120*, 215–241.

(68) Grimme, S.; Antony, J.; Ehrlich, S.; Krieg, H. A consistent and accurate ab initio parametrization of density functional dispersion correction (DFT-D) for the 94 elements H-Pu. *The Journal of chemical physics* **2010**, *132*, 154104.

(69) Grimme, S.; Ehrlich, S.; Goerigk, L. Effect of the damping function in dispersion corrected density functional theory. *Journal of computational chemistry* **2011**, *32*, 1456–1465.

(70) Neese, F. Software update: the ORCA program system, version 4.0. *Wiley Interdisciplinary Reviews: Computational Molecular Science* **2018**, *8*, e1327.

(71) Anoop, A. PyAR: Python code for Aggregation and Reaction. `https://github.com/anooplab/pyar/`, 2017.

(72) Nandi, S.; McAnanama-Brereton, S. R.; Waller, M. P.; Anoop, A. A tabu-search based strategy for modeling molecular aggregates and binary reactions. *Computational and Theoretical Chemistry* **2017**, *1111*, 69 – 81.

(73) Furche, F.; Ahlrichs, R.; Hättig, C.; Klopper, W.; Sierka, M.; Weigend, F. Turbomole. *Wiley Interdisciplinary Reviews: Computational Molecular Science* **2014**, *4*, 91–100.

(74) Becke, A. D. Density-functional exchange-energy approximation with correct asymptotic behavior. *Physical review A* **1988**, *38*, 3098.

(75) Jónsson, H.; Mills, G.; Jacobsen, K. W. Nudged elastic band method for finding minimum energy paths of transitions. **1998**,

(76) Schmidt, M. W.; Gordon, M. S.; Dupuis, M. The intrinsic reaction coordinate and the rotational barrier in silaethylene. *Journal of the American Chemical Society* **1985**, *107*, 2585–2589.

(77) Guo, Y.; Riplinger, C.; Becker, U.; Liakos, D. G.; Minenkov, Y.; Cavallo, L.; Neese, F. Communication: An improved linear scaling perturbative triples correction for the domain based local pair-natural orbital based singles and doubles coupled cluster method [DLPNO-CCSD (T)]. *The Journal of chemical physics* **2018**, *148*, 011101.

(78) Weigend, F.; Ahlrichs, R. Balanced basis sets of split valence, triple zeta valence and quadruple zeta valence quality for H to Rn: Design and assessment of accuracy. *Physical Chemistry Chemical Physics* **2005**, *7*, 3297–3305.

(79) Schlegel, H. B.; Millam, J. M.; Iyengar, S. S.; Voth, G. A.; Daniels, A. D.; Scuseria, G. E.; Frisch, M. J. Ab initio molecular dynamics: Propagating the density matrix with Gaussian orbitals. *The Journal of Chemical Physics* **2001**, *114*, 9758–9763.

(80) Schlegel, H. B.; Iyengar, S. S.; Li, X.; Millam, J. M.; Voth, G. A.; Scuseria, G. E.; Frisch, M. J. Ab initio molecular dynamics: Propagating the density matrix with Gaussian orbitals. III. Comparison with Born–Oppenheimer dynamics. *The Journal of chemical physics* **2002**, *117*, 8694–8704.

(81) Iyengar, S. S.; Schlegel, H. B.; Millam, J. M.; A. Voth, G.; Scuseria, G. E.; Frisch, M. J. Ab initio molecular dynamics: Propagating the density matrix with Gaussian orbitals. II. Generalizations based on mass-weighting, idempotency, energy conservation and choice of initial conditions. *The Journal of Chemical Physics* **2001**, *115*, 10291–10302.

(82) Frisch, M.; Trucks, G.; Schlegel, H.; Scuseria, G.; Robb, M.; Cheeseman, J.; Scalmani, G.; Barone, V.; Petersson, G.; Nakatsuji, H., et al. Gaussian 16, Revision B. 01, Gaussian Inc: Wallingford CT., 2016.[28] Lee C, Yang W, Parr RG. Development of

the colle-salvetti correlation-energy formula into a functional of the electron density. *Phys Rev B* **1988**, *37*, 785–789.

(83) Barone, V. Anharmonic vibrational properties by a fully automated second-order perturbative approach. *The Journal of chemical physics* **2005**, *122*, 014108.

(84) Chai, J.-D.; Head-Gordon, M. Long-range corrected hybrid density functionals with damped atom–atom dispersion corrections. *Physical Chemistry Chemical Physics* **2008**, *10*, 6615–6620.

(85) Krishnan, R.; Binkley, J. S.; Seeger, R.; Pople, J. A. Self-consistent molecular orbital methods. XX. A basis set for correlated wave functions. *The Journal of chemical physics* **1980**, *72*, 650–654.

(86) Clark, T.; Chandrasekhar, J.; Spitznagel, G. W.; Schleyer, P. V. R. Efficient diffuse function-augmented basis sets for anion calculations. III. The 3-21+ G basis set for first-row elements, Li–F. *Journal of Computational Chemistry* **1983**, *4*, 294–301.

(87) Baboul, A. G.; Curtiss, L. A.; Redfern, P. C.; Raghavachari, K. Gaussian-3 theory using density functional geometries and zero-point energies. *The Journal of chemical physics* **1999**, *110*, 7650–7657.

(88) Hamprecht, F. A.; Cohen, A. J.; Tozer, D. J.; Handy, N. C. Development and assessment of new exchange-correlation functionals. *The Journal of chemical physics* **1998**, *109*, 6264–6271.

(89) Stark, G. R. Reactions of cyanate with functional groups of proteins. III. Reactions with amino and carboxyl groups. *Biochemistry* **1965**, *4*, 1030–1036.

(90) Szczesniak, P.; Pazdzierniok-Holewa, A.; Klimczak, U.; Stecko, S. Synthesis of β- and γ-hydroxy α-amino acids via enzymatic kinetic resolution and cyanate-to-isocyanate rearrangement. *The Journal of Organic Chemistry* **2014**, *79*, 11700–11713.

(91) Krow, G. R. Synthesis and reactions of ketenimines. *Angewandte Chemie International Edition in English* **1971**, *10*, 435–449.

(92) Rahman, K. FORMATION OF AMINO ACID PRECURSORS UNDER EXTRATERRESTRIAL CONDITIONS (IMINES, KETENIMINE, REACTIVE, INTERMEDIATE). **1987**,

(93) De Moliner, F.; Banfi, L.; Riva, R.; Basso, A. Beyond Ugi and Passerini reactions: Multicomponent approaches based on isocyanides and alkynes as an efficient tool for diversity oriented synthesis. *Combinatorial Chemistry & High Throughput Screening* **2011**, *14*, 782–810.

(94) Kothari, A.; Zhu, L.; Babi, J.; Galant, N.; Rágyanszki, A.; Csizmadia, I. Ketene and Ammonia Forming Acetamide in the Interstellar Medium. *Journal of Undergraduate Life Sciences* **2020**, *14*, 1–1.

(95) Zhu, H.-S.; Ho, J.-J. Ab initio study of the formation of glycine via amino acetonitrile and amino-cyano-acetic acid. *The Journal of Physical Chemistry A* **2004**, *108*, 3798–3805.

(96) Hudson, R.; Moore, M. Reactions of nitriles in ices relevant to Titan, comets, and the interstellar medium: formation of cyanate ion, ketenimines, and isonitriles. *Icarus* **2004**, *172*, 466–478.

(97) Zhu, J. Recent developments in the isonitrile-based multicomponent synthesis of heterocycles. *European Journal of Organic Chemistry* **2003**, *2003*, 1133–1144.

(98) Ju, T.; Fu, Q.; Ye, J.-H.; Zhang, Z.; Liao, L.-L.; Yan, S.-S.; Tian, X.-Y.; Luo, S.-P.; Li, J.; Yu, D.-G. Selective and Catalytic Hydrocarboxylation of Enamides and Imines with CO2 to Generate α, α-Disubstituted α-Amino Acids. *Angewandte Chemie International Edition* **2018**, *57*, 13897–13901.

(99) Mita, T.; Chen, J.; Sugawara, M.; Sato, Y. One-Pot Synthesis of α-Amino Acids from Imines through CO2 Incorporation: An Alternative Method for Strecker Synthesis. *Angewandte Chemie International Edition* **2011**, *50*, 1393–1396.

(100) Abellán, T.; Chinchilla, R.; Galindo, N.; Guillena, G.; Nájera, C.; Sansano, J. M. Glycine and alanine imines as templates for asymmetric synthesis of α-amino acids. *European Journal of Organic Chemistry* **2000**, *2000*, 2689–2697.

(101) Kidwai, A. R.; Devasia, G. M. A new method for the synthesis of amino acids. Synthesis of amino acids and their derivatives through 2, 4-disubstituted 2-imidazolin-5-ones1. *The Journal of Organic Chemistry* **1962**, *27*, 4527–4531.

(102) Abbas, O.; Schulze-Makuch, D. Acetylene-based pathways for prebiotic evolution on Titan. Exo-Astrobiology. 2002; pp 345–348.